European Journal of Control 54 (2020) 64–72

Contents lists available at ScienceDirect

European Journal of Control

journal homepage: www.elsevier.com/locate/ejcon

Realization of fractional order circuits by a Constant Phase Element

A. Buscarino, R. Caponetto*, S. Graziani, E. Murgano

Dipartimento di Ingegneria Elettrica Elettronica e Informatica, University of Catania, Italy

ARTICLE INFO

Article history:
Received 12 August 2019
Revised 14 November 2019
Accepted 29 November 2019
Available online 23 December 2019

Recommended by Prof. T Parisini

Keywords:
Fractional order systems
Constant phase element
Fractional order RC circuit
Oscillator
Chaotic system

ABSTRACT

Fractional-order calculus has been used for generalizing many modern and classical control theories including the well establish PID paradigm. The obtained controllers, of non-integer order, must be approximated with high order integer ones, in order to be realized. Successively, analog or digital implementations are used for the real world applications. This approach offers the hip to a classical criticism to fractional calculus. Why design a fractional-order system, which is usually of low order, if you need a high order system to implement it? In order to face this problem, in this paper, a fractional-order capacitor, more specifically a Constant Phase Device, is applied for implementing a first order fractional transfer function. Due to the intrinsic nature of the realized device, just one capacitor is needed for the implementation, avoiding therefore the need of high order RC approximation. Furthermore a fractional-order Wien oscillator and a chaotic Duffing circuit are presented confirming the potentiality of the proposed device in realizing fractional order circuits.

1. Introduction

The subject of fractional order calculus or non integer order systems, i.e., the calculus of integrals and derivatives of any arbitrary real or complex order, has gained considerable popularity and importance during the last three decades with applications in numerous seemingly diverse and widespread fields of science and engineering, see [28,35].

Transmission lines, electrical noises, power-law, dielectric polarization, heat transfer phenomena, systems with long-range interaction, concrete, as well as biomedical engineering, are some examples of systems described by using non-integer order physical laws, see [45].

Fractional derivatives provide an excellent tool for the description of memory and hereditary properties of various materials and processes. This is one of the main advantages of fractional derivatives in comparison with classical integer-order models, in which such effects are in fact neglected, see [49].

A further interesting application of fractional calculus is in the automatic control area. CRONE control, the French acronym of Command Robuste d'Ordre Non-Entier, was the first robust control framework, based on fractional differentiation, for linear systems, see [41]. Typical system theory topics such as modeling, system identification, stability, controllability, observability and robustness now involve fractional systems as wel as controllers, see [2,12,25,26,46]. The fractional generalization of the *PID* controller, see [36], gave rise to a large number of studies and applications, see [30,31,44].

Eq. 1 represents a simple Fractional Order Controller (FOC) derived from a first order low pass filter and its implementation implies the approximation via integer order systems.

$$F(s) = \frac{k}{\left(\frac{s}{p}+1\right)^{\alpha}}, \tag{1}$$

with $\alpha \in R$.

The zeros-poles Oustaloup's approximation, see [29], is one of the most used approximation, anyway FOCs can be, actually, approximated by using analog and digital networks, see [14,16,19,37]. A update state of the art can be found in [48], where the available CMOS microelectronic technology is addressed as possible path for mass market realization of fractional order controller.

Other possible implementation of fractional order transfer function are based on Field Programmable Gate Arrays (FPGAs) and Filed Programmable Analog Arrays (FPAAs). Both methodologies have the characteristic of utilizing reprogrammable devices; in the FPGAs case the basic building block, configurable logic blocks (CLBs), are digital while in the case of FPAAs, Configurable Analog Blocks (CABs), are analog circuits. FPGAs and FPAAs are used in academies as well as in industries as initial step in VLSI design for fast testing and effective design before silicon realization. Relevant results have been addressed in see [10,17,27] using FPPAs, as well as in [1,13,20,32,39] applying the digital counterpart.

* Corresponding author.
E-mail address: riccardo.caponetto@unict.it (R. Caponetto).

https://doi.org/10.1016/j.ejcon.2019.11.009
0947-3580/

The full exploitation of FOCs he has been hindered so far by the lack of real Constant Phase Elements (CPEs) devices, i.e., devices which have an intrinsic fractional behavior. Such an issue has been actively investigated in the last few years and recently CPEs devices have been proposed in the literature.

The first CPE, called Fractor, was patented by Bohannan, see [7] and in [6] it has been applied in motor control application.

In [24] a different approach, based on Carbon Nano Tube (CNT), has been patented as possible realization of CPE.

Anyway, for CPE realization different technologies have been proposed, which can be classified as: multi-components, single components and emulated. A detailed state of the art can be found in [43].

In [11,15] the authors introduced and characterised a CPE based on Ionic Polimeric Metal Composites while, in [5,9], a CPE device realized using carbon black nano part has been introduced. This device has been utilized in the circuits proposed in this paper.

The paper is structured as follows: in Section 2 a brief introduction on Fractional Calculus is given; in Section 3 the realized fractional-order capacitor is described; Section 4 reports the applications, while in the Conclusion some final considerations are given.

2. Brief mathematical background on fractional calculus

Fractional calculus is a generalization of integration and differentiation to non-integer order fundamental operator ${}_aD_t^r$, where a and t are the limits of the operation and $r \in \mathrm{R}$, see [28,35,40]. The continuous integro-differential operator is defined as:

$$
{}_aD_t^r = \begin{cases} \frac{d^r}{dt^r} & : r > 0, \\ 1 & : r = 0, \\ \int_a^t (d\tau)^{-r} & : r < 0. \end{cases} \tag{2}
$$

The three equivalent definitions most frequently used for the general fractional derivative or integral are the Gruüwald–Letnikov (GL) definition, the Riemann–Liouville (RL) and Caputo (C) definitions.

The GL definition is given by

$$
{}_aD_t^r f(t) = \lim_{h \to 0} h^{-r} \sum_{j=0}^{[\frac{t-a}{h}]} (-1)^j \binom{r}{j} f(t - jh), \tag{3}
$$

where [.] means the integer part.

The RL definition is given as

$$
{}_aD_t^r f(t) = \frac{1}{\Gamma(n-r)} \frac{d^n}{dt^n} \int_a^t \frac{f(\tau)}{(t-\tau)^{r-n+1}} d\tau, \tag{4}
$$

for $(n-1 < r < n)$ and where $\Gamma(\bullet)$ is the *Euler Gamma* function [42].

The Caputo definition can be written as:

$$
{}_aD_t^r f(t) = \frac{1}{\Gamma(r-n)} \int_a^t \frac{f^{(n)}(\tau)}{(t-\tau)^{r-n+1}} d\tau, \tag{5}
$$

for $(n-1 < r < n)$. The initial conditions for the fractional-order differential equations with the Caputo derivatives are in the same form as for the integer-order differential equations. In the above definition, $\Gamma(m)$ is the factorial function.

Modeling of non-integer order electronic devices is needed for the one proposed in this paper.

Resistors (R), inductors (L) and capacitors (C) are electric passive circuit elements, whose impedances are given by:

$$
Z(s) = Ks^{-\alpha} \tag{6}
$$

where K is a gain, s represents the Laplace variable and $\alpha \in \{-1,0,1\}$ the order for inductor, resistor and capacitor, respectively.

The impedance is described in the frequency domain by substituting $j\omega$ for s, where j is the imaginary unit and ω is the angular frequency.

The impedance then becomes:

$$
Z(j\omega) = K(j\omega)^{-\alpha} \tag{7}
$$

The magnitude and phase of this impedance are $|Z| = K/\omega^{\alpha}$ and $Arg(Z) = -\alpha\pi/2$, respectively. For $\alpha \in$ {-1,0,1}, the phase is $\pi/2$ (i.e., inductor), 0 (i.e., resistor), and $-\pi/2$ (i.e., capacitor), respectively.

According to (7) a fractional element exhibits a constant-phase behavior and is often referred as a CPE. CPE realization and applications can be found in [4,18] and [3,21].

The availability of fractional-order capacitor with constant phase in an as large as possible frequency range will play a fundamental role in the possibility of realizing non-integer order controller.

3. Materials and device realization

In [5,9], some of the authors have demonstrated the feasibility of fabricating CPEs by using Carbon Black (CB), dispersed in a polymeric matrix, see also Fig. 1.

Devices fabricated in [9] were realized using Sylgard, as polymeric matrix, and CB as dispersed filler, so that nanostructured devices were obtained. Also, the possibility of controlling the nature of the FOEs characteristics, by changing some fabrication process parameters (CB percentage, curing time and curing temperature), was suggested.

Sylgard$_{184}$ has been used for realizing the polymeric matrix of the capacitor dielectric. It was purchased from *DowCorning* as a two part liquid elastomer kit. Part A (consisting in the vinyl-terminated PDMS prepolymer), and Part B (the crosslinking curing agent, consisting in a mixture of methylhydrosiloxane copolymer chains with a Pt catalyst and an inhibitor).

CB (acetylene, 100% compressed, 99.9%, specific area 75 m^2/g, bulk density $170-230$ g/L, average particle size 0.042 µm) was purchased from *AlfaAesar* and used as received. The described CB based composite material is the dielectric of the capacitances investigated in the following of the paper. The resulting structure of the CB-FOE is given in Fig. 2.

The CB-FOE samples have been prepared by mixing the *PDMS* and the crosslinking agent in a weight ratio of 1:10 in a Teflon crucible. The mixture was mixed for 10 min. CB has been added for achieving the desired concentration. The mixture was stirred for further 10 min for enhancing the dispersion of the CB.

Curing at different temperatures were carried out, taking into account both the manufacturer recommended curing time and the heat propagation through the mold. This results in a stabilization time, required for the temperature of the curing *PDMS* approaching the desired curing temperature. The mixture was used for realizing the capacitors dielectric by pouring the viscous mixture into the device. The mixture was allowed to crosslink at room temperature, or in an oven preheated to the desired temperature, for 48 h. More specifically, the obtained dielectrics have been used to realize cylindrical capacitors, whose geometry is shown in Fig. 2. Capacitances considered in the following had copper-based shell with height $h = 8$ cm, internal diameter $a = 0.6$ cm and external diameter $b = 1.2$ cm. The curing time was 53 min at 100 °C, 38 min at 125 °C, and 28 min at 150 °C.

So far, for the devices realized in [9], no relevant changes have been observed on its pseudo-capacitance value nor on its fractional-order, giving evidence of good stability.

In Fig. 3, the Bode diagrams of the applied fractional order capacior is reported. The frequency response has been obtained by using a spectrum analyzer Keysight Technologies E5061B. The

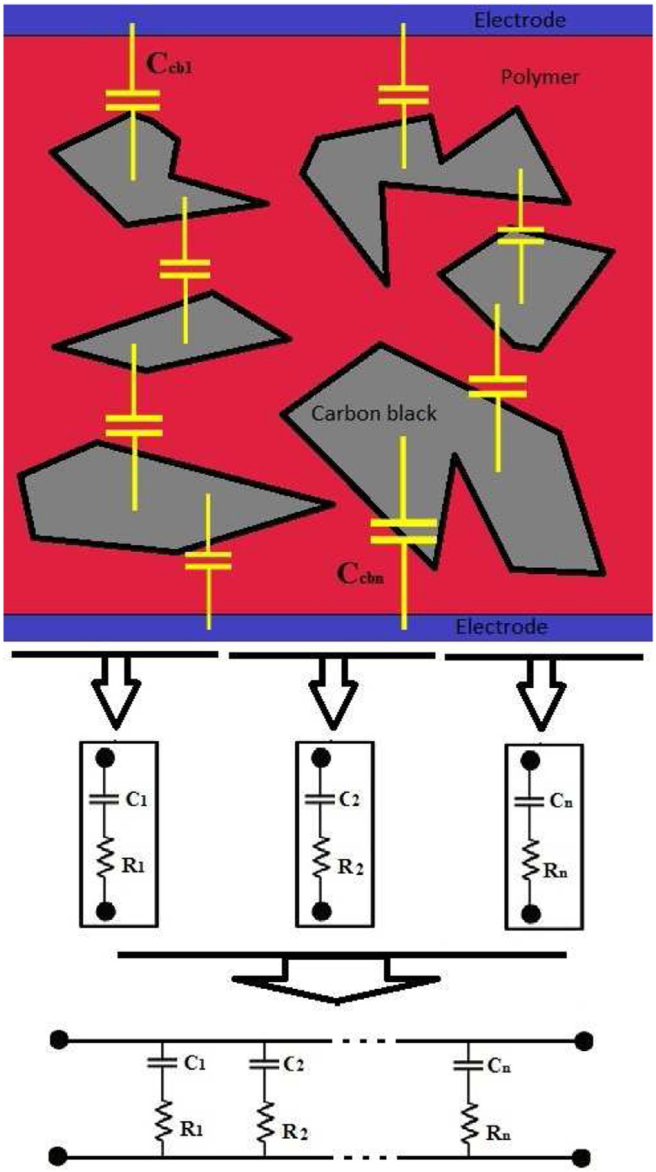

Fig. 1. Structure of CB based FOE. Carbon black dispersed inside the polymer.

Fig. 2. Realized CB-FOE.

values of α and the pseudo capacitance C of the considered device are respectively: $\alpha = 0.81$ and $C = 2.7\,\text{nF}$.

4. Circuits realization

In this section three applications of the described device are reported. The first one is the realization of a simple fractional-order transfer function realized with the CPE and one resistor. The second is a Wien oscillator. The proposed realization is a fractional-order generalization of the classical Wien oscillator. The last realization is a Duffing chaotic system. Duffing system has been implemented using two differential equations whose order is less then two. The circuit shows the expected characteristic chaotic behavior.

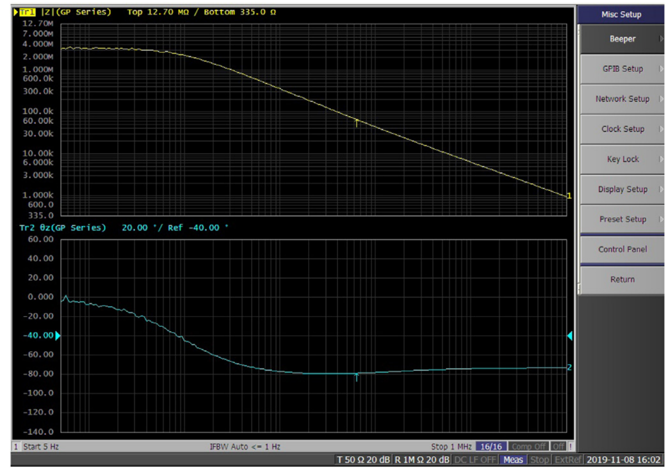

Fig. 3. Bode diagram of the $CB - FOE$ 140B.

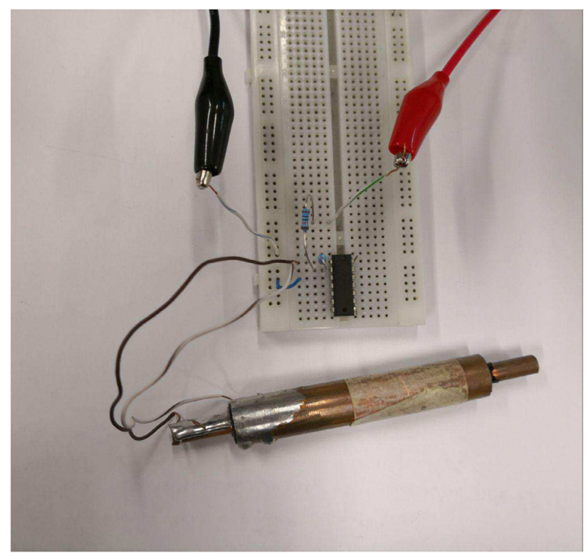

Fig. 4. Fractional order *RC* circuit.

4.1. Fractional-order transfer function via RC$^{\alpha}$ filter

The passive circuit has been realized with a resistor $R = 100\ k\Omega$ and a non-inverting buffer output stage, while the active filter adding the operational amplifier *TL*084 in inverting real integrator configuration with $R_1 = R_2 = 100\ \text{k}\Omega$. The circuit is shown in Fig. 4.

The response of both circuits have been compared with the analytical solution of the following fractional-order differential equation representing a *RC* circuit of order α:

$$\frac{d^{\alpha}y(t)}{dt^{\alpha}} = -\frac{1}{RC}y(t) + \frac{1}{RC}u(t) \tag{8}$$

The equation has been integrated by using the procedure introduced in [22].

The comparison between the measured and analytical responses is shown in Fig. 5.

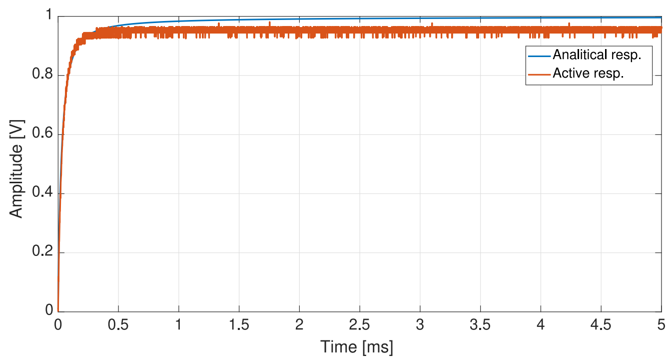

Fig. 5. Comparison of the step response between active circuit implementation and the simulated one for fractional order *RC* output.

The order α of the $CB-FOE$ 140B has been previously fixed taking into account the slope of the magnitude of the Bode diagram reported in Fig. 3, and confirmed by the constant value of the phase. The obtained value is $\alpha = 0.81$.

Once the value of α has been fixed to 0.81 and the value of R to 100 kΩ, relation 8 has been used to find the value of C that fits the measured and simulated data. This value, $C = 2.7$ nF, corresponds to the pseudo-capacitance of the $CB-FOE$ 140B.

The difference of few mV shown in Fig. 6 between the passive and active filters is due to an offset of the operational amplifier.

As a further comparison an integer-order RC filter with a commercial capacitance of value $C = 2$ nF as close as possible to a value of the pseudo capacitance $CB-FOE$ 140B has been realized and the measured outputs are compared.

In Fig. 7 it is possible to note the effect of fractional-order derivative both in the transient as well as in the steady state regime.

4.2. Fractional-order oscillator

As it is well known, a generic system (both integer-order and fractional-order) must have some important properties to be able to generate oscillations: a system order greater or equal than two and nonlinearities in its definitions; if these conditions are not fulfilled the system cannot oscillate. The first property can be easily achieved using systems with at least two state-space variables (e.g. two capacitors in analog circuits). For the second property, some nonlinearities must be included inside the mathematical model and then physically realized (e.g. in a lot of analog applications operational amplifiers saturation is used as nonlinearity). According to [38] a general fractional-order Barkhausen oscillation conditions for FOSs with two or three state-space variables and different fractional-orders can be obtained.

In the following subsection a brief analysis on Wien oscillator is done and then simulation and implementation results are shown.

4.2.1. Wien oscillator

The electronic circuit is shown in Fig. 8 and both C_1 and C_2 are FOEs with orders $\alpha,\ \beta \in \mathbb{R}$ respectively.

As reported in [38], state space equations (whose variables are V_{C_1} and V_{C_2}) are the following:

$$\begin{bmatrix} \dfrac{dV_{C_1}^{\alpha}}{dt^{\alpha}} \\ \dfrac{dV_{C_2}^{\beta}}{dt^{\beta}} \end{bmatrix} = \begin{bmatrix} \dfrac{a-1}{R_4C_1} - \dfrac{1}{R_3C_1} & -\dfrac{1}{R_4C_1} \\ \dfrac{a-1}{R_4C_2} & -\dfrac{1}{R_4C_2} \end{bmatrix} \begin{bmatrix} V_{C_1} \\ V_{C_2} \end{bmatrix} + \begin{bmatrix} \dfrac{b}{R_4C_1} \\ \dfrac{b}{R_4C_2} \end{bmatrix}, \tag{9}$$

where

$$(a, b) = \begin{cases} (0, V_{sat}) & KV_{C_1} \geq V_{sat} \\ (K, 0) & -V_{sat} < KV_{C_1} < V_{sat} \\ (0, -V_{sat}) & -V_{sat} \geq KV_{C_1} \end{cases}. \tag{10}$$

In Eq. (9), $K = 1 + R_1/R_2$ is the gain of the operational amplifier (which is fundamental to stabilize the circuit) and V_{sat} is its saturation voltage. Analyzing state-space circuit equations it's clear that (a, b) represents the circuit nonlinearity, which depends on amplifier's saturation.

Supposing to have different passive components (i.e. $R_3 \neq R_4$, $C_1 \neq C_2$ and $\alpha \neq \beta$) and Barkhausen oscillation conditions are satisfied, the oscillation pulsation ω and frequency f are equal to:

$$\omega = \left(\frac{1}{R_3R_4C_1C_2}\right)^{\dfrac{1}{\alpha+\beta}} \rightarrow f = \frac{\omega}{2\pi} \tag{11}$$

In the common used integer-order case (i.e. $\alpha = \beta = 1$, $R_3 = R_4 = R$ and $C_1 = C_2 = C$), the pulsation frequency is equal to $\omega = 1/\sqrt{RC}$ while in this general case it depends even on α and β and so it is possible to exploit a wider frequency range domain and high frequency sinusoidal waves can be generated. Following the design procedure reported in [38] another important issue involves the gain K: in the common integer-order case it must be greater

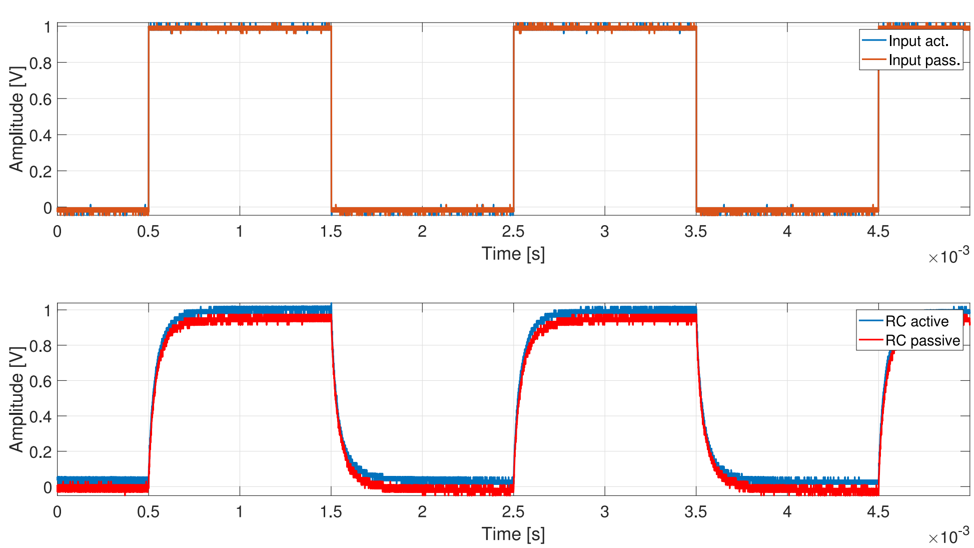

Fig. 6. Comparison between passive and active circuit implementation of the fractional order *RC* output.

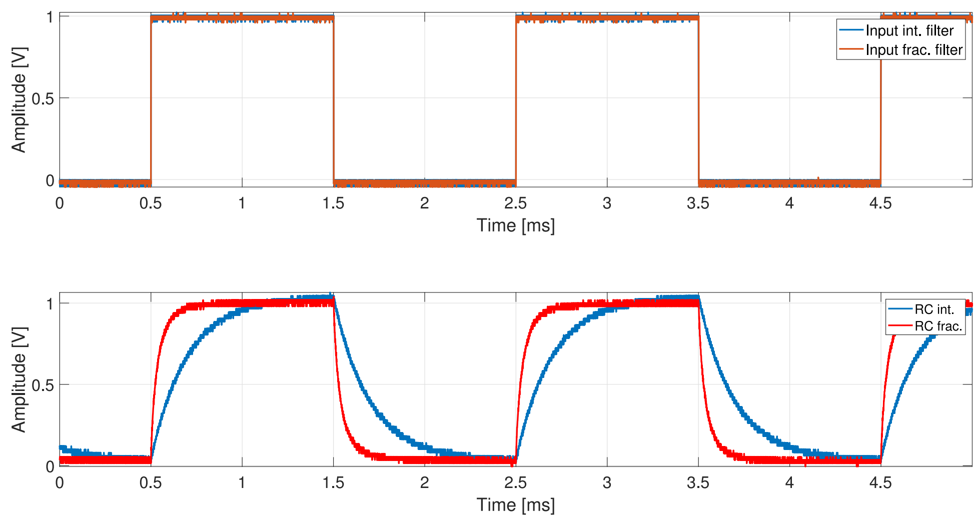

Fig. 7. Comparison between integer and fractional order *RC* outputs.

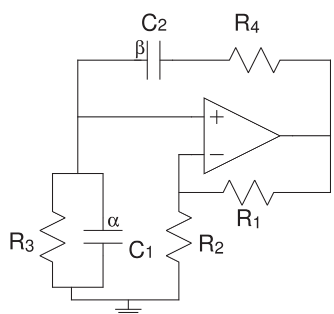

Fig. 8. Fractional order Wien oscillator schematics.

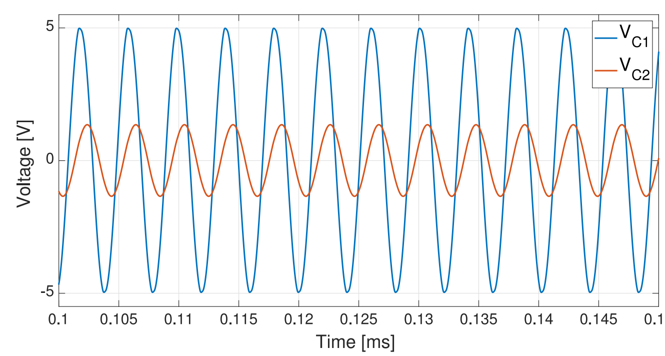

Fig. 9. Voltage on the two capacitor of the Wien oscillator. MATLAB simulation.

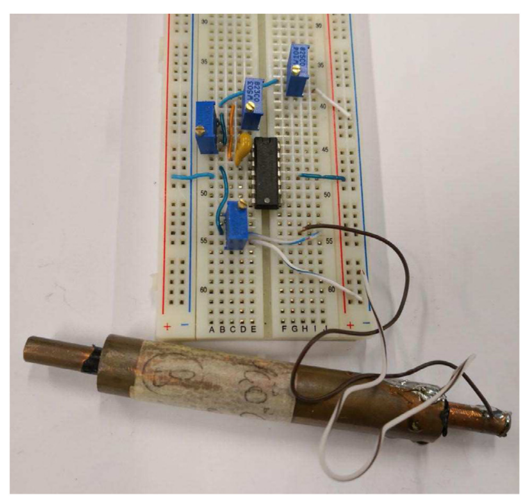

Fig. 10. Fractional-order Wien oscillator realization.

or equal than three to start and maintain oscillations while in the fractional-order case can be less than three.

In the following, experimental results are presented.

In this case study, both in simulation and real implementation design, the following parameters are considered:

where C_1 is the FOE discussed before. Resistor values are chosen according to design procedure of [38] and are the following: $R_1 = 14.05$ kΩ, $R_2 = 33$ kΩ (this is arbitrary chosen), $R_3 = 4.17$ kΩ and $R_4 = 0.78$ kΩ. The gain $K = 1.42$ shows that sustained oscillations are obtained with a gain less than the integer-order case counterpart.

Supposing for each capacitor an initial condition equal to 5 V, simulation results are obtained in MATLAB environment, by using the integration routines introduced in [22] and here reported in Fig. 9.

The aforementioned parameters are used to build the fractional-order Wien oscillator. It is possible to see that with only one FOE a fractional-order oscillator can be obtained. In particular, high-frequency oscillations are generated considering the frequency range of the capacitor C_1 where it behaves as CPE.

In Fig. 10 the analog implementation of the Wien oscillator is presented, where trimmers are used instead of classical resistors.

In the integer-order case, it is well known that to start oscillations is necessary a gain different from the nominal one (i.e., $K = 3$) and, in any case, some mismatch among the nominal frequency and the real one arises. Using parameter values obtained with the design procedure, it has been necessary increase R_2 value to start oscillations. To overcome this problem, gain K has been experimentally changed and for $K_{real} = 1.39$ setting $R_2 = 35.8\,\mathrm{k}\Omega$ a sinusoidal oscillation is obtained and shown in Fig. 11.

In Fig. 12 the voltage of fractional-order capacitor is measured and compared with the one obtained in simulation.

Neglecting the phase-shift, due to different starting point of the two waves, a difference in the amplitude between the two signals is evident. In order to investigate this effect a Fast Fourier Transform of the simulated and real signals has been performed. The

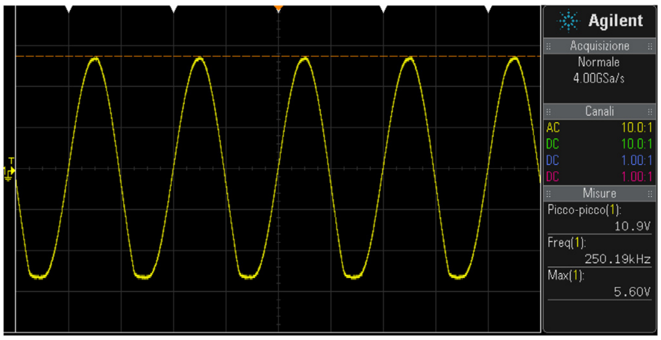

Fig. 11. f Fractional-order Wien oscillator sinusoidal wave @ 250 kHz, C_1 voltage.

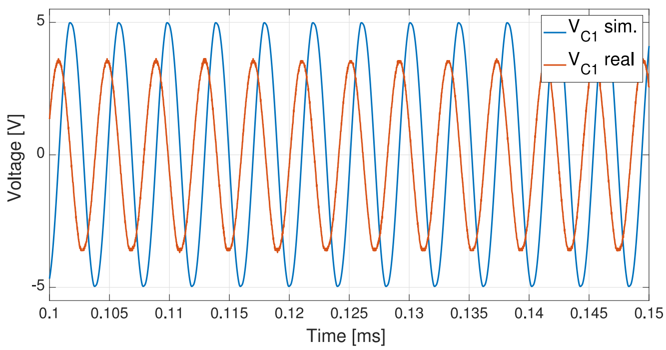

Fig. 12. Simulated and real fractional-order C_1 voltage.

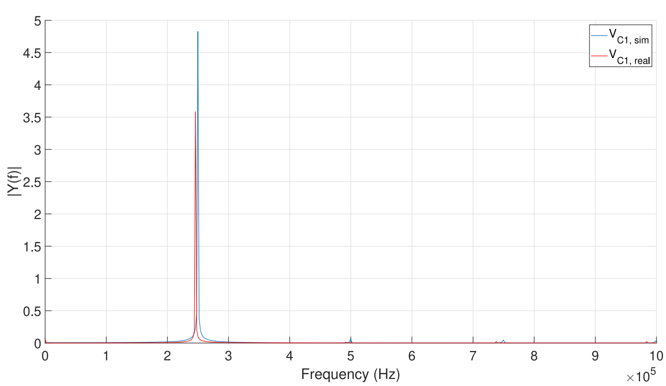

Fig. 13. FFT of simulated and real fractional-order C_1 voltage.

result, see Fig. 13 confirm that the fractional order Wien circuit oscillates at the desired frequency. The discrepancy in amplitude has been investigated realizing, with the CB140B, an RLC circuit with $R = 1\,\mathrm{k}\Omega$ and $L = 4.7\,\mathrm{mH}$. In Fig. 14 the oscillation of the RLC circuit at 300 kHz is shown. Also in this case a reduction in the amplitude is evident. The discrepancy can be addressed as effect of non modelled phenomena in the fractional capacitor that need further investigation.

4.3. Fractional-order Duffing System

Duffing system [33,47] is a well known and studied system: it is a second order driven nonlinear system able to show a wide range of different dynamical behavior, i.e. from periodic oscillations to chaos, if opportunely excited. The following equations represent the dynamical equations to which the above-mentioned sys-

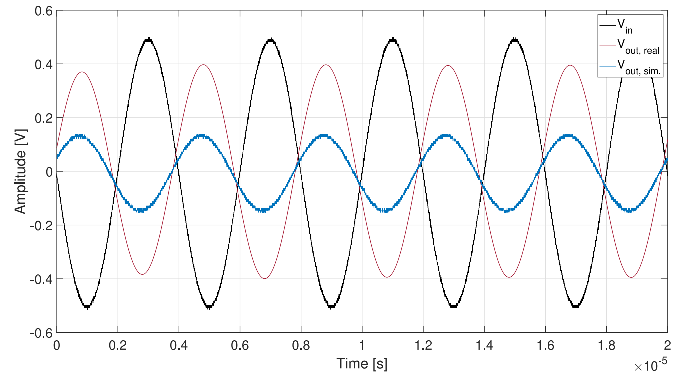

Fig. 14. OScillation at 250 kHz of the RLC fractional circuit.

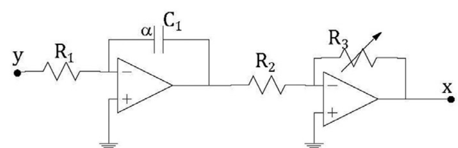

Fig. 15. Analog realization of first equation of the FO-Duffing system with the discussed FOE.

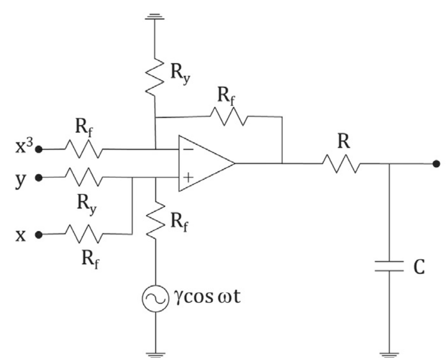

Fig. 16. Analog realization of second equation of the FO-Duffing system with an integer-order integrator.

tem obeys:

$$\begin{cases} \dfrac{dx}{dt} = y, \\ \dfrac{dy}{dt} = x - x^3 - \delta y + \gamma \cos \omega t \end{cases} \tag{12}$$

These equations represent a *RLC* circuit excited by a sinusoidal voltage source when the capacitor C has a nonlinear cubic characteristic in the q-v plane. Eq. (12) encompasses a number of system parameters, namely δ, γ, and ω, which may act as bifurcation parameters. In particular, the amplitude and the frequency of the driving signal assume a relevant role in selecting the emerging dynamical behavior. Fixing δ, γ, and varying the frequency ω it is possible to drive the system towards a period-doubling bifurcation cascade leading to a double-scroll-like chaotic attractor.

The possibility of realizing fractional-order systems has been demonstrated in literature. The first approach is based on evaluating the fractional-order derivatives for all the system's state-space variables, see [23]; the other one by evaluating only one fractional-order derivative of all the state-space variables, see [34].

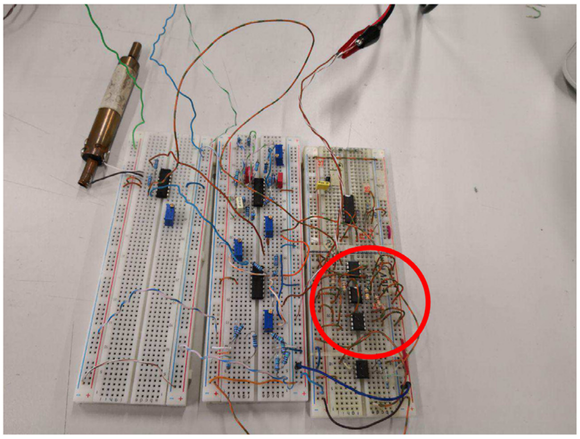

Fig. 17. Circuit implementation of FO-Duffing System with order $\alpha = 0.81$.

In [8], similarly, a strategy for designing fractional order systems showing jump resonance is presented along with the procedure to design and implement an analog circuit based on the approximation of the fractional order derivative. In this paper, the former approach has been considered to obtain a fractional-order Duffing system.

According to Eq. (12), its fractional-order counterpart can be considered simply evaluating the α-order derivative of the x variable.

Considering $0 < \alpha < 1$, the FO-Duffing system is represented by the following equations:

$$\begin{cases} \dfrac{d^\alpha x}{dt^\alpha} = y, \\ \dfrac{dy}{dt} = x - x^3 - \delta y + \gamma \cos \omega t \end{cases} \tag{13}$$

In this case the total system order is equal to $\alpha + 1 < 2$ and of course if $\alpha = 1$ then Eq. (13) corresponds to Eq. (12). In this application, the discussed FOE is used to proof that chaos can be generated with a total system order less than 2, in particular the order will be 1.81 because $\alpha = 0.81$.

The first equation is represented by the following electronic schematics, where $R_1 = R_2 = 10\ k\Omega$ and R_3 is a variable resistance, whose value is fixed to $R_3 = 8.8\ \text{k}\Omega$.

In the following schematics is presented the analog realization of the entire FO-Duffing system, where $R_f = 100\ \text{k}\Omega$, $R_y = 80\ \text{k}\Omega$, $R = 10\ \text{k}\Omega$ and $C = 10$ pF.

The circuital implementation of 1.81-order Duffing system is finally shown in the next figure.

Starting from the left, the circuits reported in Figs. 15 and 16 have been implemented respectively in the first and in the second breadboard; while on the third one the analog implementation of the cubic power of the x variable is realized (inside the red circle).

This latter has been realized with two *AD-366* multipliers and two opamps. The schematics is reported in Fig. 18. In particular, resistance values are the following: $R_1 = R_3 = 10\ \text{k}\Omega$ and $R_2 = R_4 = 100\ \text{k}\Omega$.

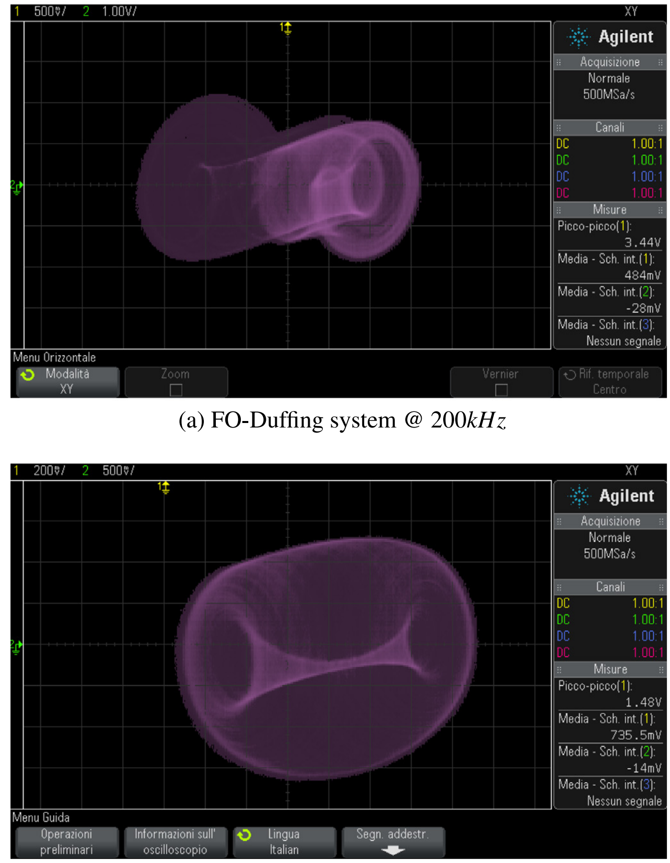

(a) FO-Duffing system @ $200kHz$

(b) FO-Duffing system @ $300kHz$

Fig. 19. FO-Duffing system excited at different frequencies that determine chaotic dynamics.

Table 1
Wien circuit parameters.

α	0.81
C_1	2.7 nF
β	1
C_2	1 nF
f	250 kHz
V_{cc}	± 7 V

As a forcing input a sine wave with a peak to peak amplitude of 4 V has been chosen. Figs. 19 and 20 show the acquired attractors from the realized circuit, excited with different frequencies. The double-scroll-like shape of the Duffing attractor is obtained with an exciting frequency equal to 200 kHz, while increasing to $f = 300$ kHz the circuit goes toward a torus surrounding the original attractor, Fig. 19b, then at a frequency $f = 500$ kHz the torus collapses around an internal limit cycle, Fig. 20a, to which it stabilizes at a frequency $f = 800$ kHz, Fig. 20b.

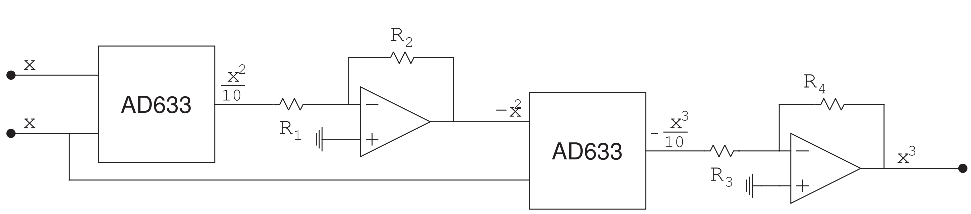

Fig. 18. Analog realization of cubic multiplier.

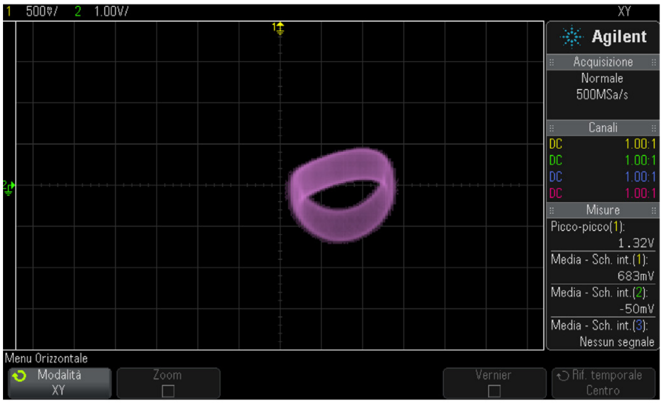

(a) FO-Duffing system @ 500kHz

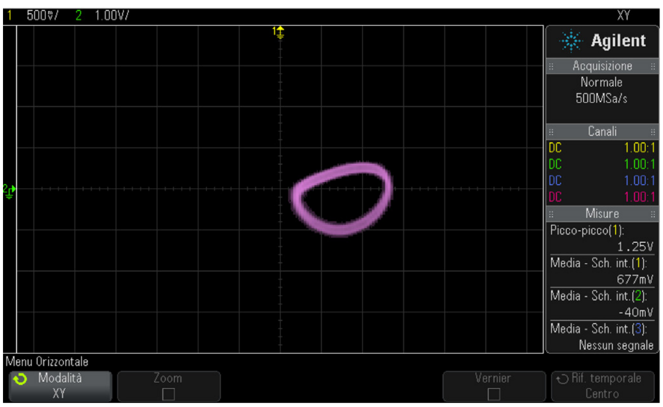

(b) FO-Duffing system @ 800kHz

Fig. 20. FO-Duffing system excited at different frequencies that determine limit cycles.

5. Conclusions

In this paper CPE, fabricated by using a carbon black nanostructured dielectrics, has presented and utilized as capacitor for the realization of three fractional-order circuits. A fractional first order transfer function realized via an RC^{α} filter, a Wien oscillator and a chaotic Duffing system have been presented. The obtained results are encouraging and let foresee for a possible application of these devices in analog fractional order controllers. So far, no relevant changes have been observed on the pseudo-capacitance value of the realized device nor on its fractional order, giving evidence of good stability. Further research activities are going to be developed to produce stable and well characterized devices with a constant-phase frequency window as greater as possible. Moreover, where fractional order chaos control strategies are outlined, there are no attempt of a physical implementation. A further future activity will be the application of the device presented in this paper for implementing real systems fractional order chaos control laws.

Declaration of Competing Interest

We declare that none of the authors don't have any conflict of interest with the respect of the manuscript entitled 'Realization of Fractional Order Transfer Function via Constant Phase Element' contents.

References

[1] L.F. Ávalos-Ruiz, C.J. Zúñiga Aguilar, J. F. Gómez-Aguilar, R. F. Escobar-Jiménez, H. M. Romero-Ugalde, FPGA implementation and control of chaotic systems involving the variable-order fractional operator with Mittag-Leffler law, Chaos Solitons Fractal 115 (2018) 177–189.
[2] B. Bandyopadhyay, S. Kamal, Stabilization and Control of Fractional Order Systems: a Sliding Mode Approach, Springer, Heidelberg, 2015 317, doi:10.1007/978-3-319-08621-7.
[3] K. Biswas, S. Sen, K. Dutta, A constant phase element sensor for monitoring microbial growth, Sensors Actuators 191 (2006a) 186–191.
[4] K. Biswas, S. Sen, K. Dutta, Realization of a constant phase element and its performance study in a differentiator circuit, IEEE Trans. Circuit Syst.-II 53 (9) (2006b) 802–806.
[5] K. Biswas, R. Caponetto, G.D. Pasquale, S. Graziani, A. Pollicino, E. Murgano, Realization and characterization of carbon black based fractional order element, Microelectron. J. 82 (2018) 22–28, doi:10.1016/j.mejo.2018.10.008.
[6] G. Bohannan, Analog fractional order controller in temperature and motor control applications, J. Vib. Control 14 (2008) 1487–1498.
[7] G. Bohannan, S. Hurst, L. Spangler, Electrical component with fractional order impedance, Patent reference WO2006112976A3. Filling date 1003/2016.
[8] A. Buscarino, R. Caponetto, C. Famoso, L. Fortuna, Jump resonance in fractional order circuits, Int. J. Bifurc. Chaos 28 (1) (2018).
[9] A. Buscarino, R. Caponetto, G.D. Pasquale, L. Fortuna, S. Graziani, A. Pollicino, Carbon black based capacitive fractional order element towards a new electronic device, Int. J. Electron. Commun. (AEÜ) 84 (2018) 307–312.
[10] R. Caponetto, G. Dongola, Field programmable analog array implementation of non integer order *PID* controller, Trans. ASME J. Comput. Nonlinear Dyn. 3 (2) (2008) 1–8.
[11] R. Caponetto, G. Dongola, L. Fortuna, S. Graziani, S. Strazzeri, A fractional model for IPMC actuators, in: Proceedings of the IEEE Instrumentation and Measurement Technology Conference, pp. 2103–2107. Art. no. 4547395.
[12] R. Caponetto, G. Dongola, L. Fortuna, I. Petrás, Fractional order systems - modeling and control applications, vol. 72, in: Proceedings of the World Scientific Series on Nonlinear Science Series, 2010.
[13] R. Caponetto, G. Dongola, A. Gallo, Fractional integrative operator and its FPGA implementation, Proceedings of the ASME International Design Engineering Technical Conferences and Computers and Information in Engineering Conference 4 (2009) 1285–1291. DETC2009.
[14] R. Caponetto, G. Dongola, G. Maione, A. Pisano, Integrated technology fractional order proportional-integral-derivative design, J. Vib. Control 20 (7) (2014) 1066–1075.
[15] R. Caponetto, S. Graziani, F. Pappalardo, F. Sapuppo, Experimental characterization of ionic polymer metal composite as a novel fractional order element, in: Proceedings of the Advances in Mathematical Physics, 2013, doi:10.1155/2013/953695.
[16] R. Caponetto, P. Lino, G. Maione, V. Tomasello, Design and efficient implementation of digital non-integer order controllers for electro-mechanical systems, J. Vib. Control 22 (9) (2016).
[17] R. Caponetto, D. Porto, Analog implementation of non integer order integrator via field programmable analog array, IFAC Proc. 2 (2006) 107–111.
[18] S. Das, M. Sivaramakrishna, K. Biswas, B. Goswami, Performance study of a constant phase angle based impedance sensor to detect milk adulteration, Sensors Actuators 167 (2011) 273–278.
[19] R. De Keyser, C. Muresan, C. Ionescu, An efficient algorithm for low-order direct discrete-time implementation of fractional order transfer functions, ISA Trans. 74 (2018) 229–238.
[20] A.J.A. El-Maksoud, A.A.A. El-Kader, B. G. Hassan, N. G. Rihan, M. F. Tolba, L. A. Said, A. G. Radwan, M.F. Abu-Elyazeed, FPGA implementation of sound encryption system based on fractional-order chaotic systems, Microelectron. J. 90 (2019) 323–335.
[21] M. Elshurafa, N. Almadhoun, K. Salama, H. Alshareef, Microscale electrostatic fractional capacitors using reduced graphene oxide percolated polymer composites, Appl. Phys. Lett. 102 (2013) 23.
[22] R. Garrappa, Trapezoidal methods for fractional differential equations: theoretical and computational aspects, Math. Comput. Simul. 110 (2015) 96–112.
[23] T.T. Hartley, C.F. Lorenzo, H.K. Qammer, Chaos in a fractional order Chua's system, IEEE Trans. Circ. Syst. 42 (8) (1995) 485–490.
[24] D. John, S. Banerje, K. Biswas, A CNT-epoxy nanoparticle based fractional capacitor and a method for fabricating the same. Application No: 201631042210. Patent filed in 2016.
[25] Y. Luo, Y.Q. Chen, Fractional Order Motion Control, J. Wiley & Sons, 2013.
[26] C.A. Monje, Y.Q. Chen, B.M. Vinagre, D. Xue, V. Feliu, Fractional Order Systems and Control, Springer, London, 2010.
[27] C. Muñiz Montero, L.V. Garcí-Jiménez, L.A. Sãnchez Gaspariano, et al., New alternatives for analog implementation of fractional-order integrators, differentiators and $p^{\lambda} i^{d}$ controllers based on integer-order integrators, Nonlinear Dyn. 90 (241) (2017), doi:10.1007/s11071-017-3658-z.
[28] K.B. Oldham, J. Spanier, The fractional calculus: theory and applications of differentiation and integration to arbitrary order, in: Dover Books on Mathematics, 2006.
[29] A. Oustaloup, F. Levron, B. Mathieu, F.M. Nanot, Frequency band complex noninteger differentiator: characterization and synthesis, IEEE Trans. Circuits Syst. I: Fundam. Theory Appl. 47(200) 25–39. (1).
[30] H. Özbay, C. Bonnet, A. Fioravanti, PID controller design for fractional-order systems with time delays, Syst. Control Lett. 61 (2012) 18–23.
[31] F. Padula, A. Visioli, Tuning rules for optimal PID and fractional-order PID controllers, J. Process Control 21 (1) (2011) 69–81.
[32] A. Pano-Azucena, B. Ovilla-Martinez, E. Tlelo-Cuautle, J.M. Muñoz Pacheco, L.G. de la Fraga, FPGA-based implementation of different families of frac-

tional-order chaotic oscillators applying Grünwald-Letnikov method, Commun. Nonlinear Sci. Numer. Simul. 72 (2019) 516–527.
[33] T.S. Parker, L.O. Chua, Chaos: a tutorial for engineers, Proc. IEEE 75 (8) (1987) 982–1008.
[34] I. Petráš, Control of fractional-order Chua's system, J. Electr. Eng. 53 (2002) 219–222.
[35] I. Podlubny, Fractional differential equations. an introduction to fractional derivatives, fractional differential equations, in: Some Methods of Their Solution and Some of Their Applications, Academic Press, 1999.
[36] I. Podlubny, Fractional-order systems and $PI^{\lambda}d^{\mu}$ controllers, IEEE Trans. Autom. Control 44 (1) (1999) 208–214.
[37] A. Radwan, K.N. Salama, Fractional-order RC and RL circuits, Circuits Syst. Signal Process. 31 (6) (2012).
[38] A.G. Radwan, A. Elwakil, A.M. A. M. Soliman, Fractional-order sinusoidal oscillators: Design procedure and practical examples, IEEE Trans. Circuits Syst. 55 (7) (2008) 2051–2063.
[39] K. Rajagopal, S. Jafari, S. Kacar, A. Karthikeyan, A. Akgül, Fractional order simple chaotic oscillator with saturable reactors and its engineering applications, Inf. Technol. Control 48 (2019).
[40] B. Ross, Fractional Calculus and its Applications, Springer-Verlag, 1975.
[41] J. Sabatier, C. Farges, A. Oustaloup, Fractional Order Differentiation and Robust Control Design, Springer, Dordrecht, 2015.
[42] P. Sebah, X. Gourdon,. Available online at, Introduction to the gamma functions, 2002, http://numbers.computation.free.fr/Constants/constants.html.
[43] Z.M. Shah, M.Y. Kathjoo, F.A. Khanday, K. Biswas, C. Psychalinos, A survey of single and multi-component fractional-order elements (FOEs) and their applications, Microelectron. J. 84 (2019) 9–25.
[44] P. Shaha, S. Agasheb, Review of fractional PID controller, Mechatronics 38 (2016) 29–41.
[45] H. Sun, Y. Zhang, D. Baleanu, W. Chen, Y. Chen, A new collection of real world applications of fractional calculus in science and engineering, Commun. Nonlinear Sci. Numer. Simul. 64 (2018) 213–231.
[46] A. Tepljakov, Fractional-order Modeling and Control of Dynamic Systems, Springer, 2017.
[47] J.M.T. Thompson, H.B. Stewart, Nonlinear Dynamics and Chaos, John Wiley & Sons, 1986.
[48] G. Tsirimokou, C. Psychalinos, A. Elwakil, Design of CMOS Analog Integrated Fractional-Order Circuits Applications in Medicine and Biology, Springer, Briefs in Electrical and Computer Engineering, 2017.
[49] V. Uchaikin, Fractional derivatives for physicists and engineers, in: Nonlinear Physical Science, Springer, 2013.